Origin(s) and Evolution of KREEP Basalts

Karl Cronberger[1] and Clive R Neal[1] [1]Department of Civil & Env. Eng. & Earth Sciences, University of Notre Dame. [1]kcronber@nd.edu, [2]cneal@nd.edu.

Introduction: The chemical signature KREEP [representing enrichment in potassium [K], rare-earth elements [REE], phosphorus [P], and other incompatible trace elements [ITE]) has been found at every Apollo sample return site from the Moon. It is derived from the last dregs of liquid from the lunar magma ocean known as primordial KREEP or urKREEP [1]. Pure urKREEP is not found within the sample collection, instead it is found diluted within KREEP basalts.

KREEP basalts are distinct from mare basalts by having a lower Ca/Al ratio reflected in a paucity of high-Ca pyroxene [2]. Unlike the KREEP chemical signature, KREEP basalts have only been recovered from the Apollo 14, 15 and 17 sites.

KREEP basalts are the result of endogenous melting of the lunar interior (e.g. [3]), or can be formed by homogenization of KREEP and surrounding lithologies by impact melting (e.g. [4]). Early methods to test these two hypotheses used highly siderophile element abundances (e.g. [5]), but were not without issue [6]. Recently, quantitative petrographic methods have been used to determine between the endogenous or impact origins for KREEP basalts and other lunar samples [7,8].

Through utilizing in situ major and trace element analyses, petrographic observations, and element mapping we evaluate the petrogenesis of KREEP basalts using samples 14073,16; 14155,11; 14160,214; 14310,25; 14431,2; 15205,110; 15243,6 ,43 ,60; 15382,6; 15386,3; 15434,181; and 72275,136.

Methods: Electron Probe Micro Analysis (EPMA) on the samples was conducted using a JEOL JXA-8200 microprobe and a Cameca SX-50. In total 736 pyroxenes, and 324 plagioclase analyses were conducted (data for 14160,214 and 15434,181 are from [9], and [10] respectively).

Trace elements were analyzed at Notre Dame's Midwest Isotope and Trace Element Research Analytical Facility (MITERAC) using a Thermo Scientific Element 2 high-resolution magnetic sector ICP-MS and a New Wave UP213 laser system. Laser Ablation Inductively Coupled Plasma Mass Spectrometry (LA-ICP-MS) analyses were carried out. The external standard used was the NIST 612 glass [11] and Calcium (determined by EPMA) was used as an internal standard. Sixty-six pyroxenes, and thirty-seven plagioclase analyses were carried out by LA-ICP-MS.,

Trace-element data were used to calculate equilibrium liquid compositions. Partition coefficients were calculated for pyroxene and plagioclase using the models of [12] and [13] for pyroxene, and [14] and [15] for plagioclase. These models are temperature sensitive, so defining an appropriate temperature is necessary to produce precise and accurate data. Following previous work [10] we calculated pyroxene crystallization temperatures using the methods of [16].

Results: Pyroxene compositions (Fig. 1) within the Apollo 14 KREEP basalts, progress from enstatite-rich (Mg# = 85) to a more augitic composition. However,

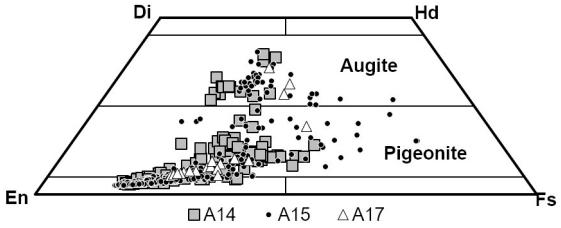

Fig 1: Pyroxene quadrilateral of analyzed KREEP basalts.

samples 14073,16, 14155,11, and 14160,214 also progress into a more Fe-rich pigeonite composition with 14073,16 possessing a single pyroxferroite analysis. Pyroxenes from the Apollo 15 KREEP basalts trend from enstatite (Mg# = 87), to Mg-rich pigeonite to augite and Fe-rich pigeonite. The pyroxenes of Apollo 17 KREEP basalts are distinctive in that no enstatite compositions were recorded. The most primitive pyroxenes are Mg-rich pigeonites (Mg# = 74.3) that become more Fe-rich. There is an apparent gap between the pigeonites and the augitic pyroxenes (but this may be a sampling issue).

Plagioclases within the KREEP basalts are typically

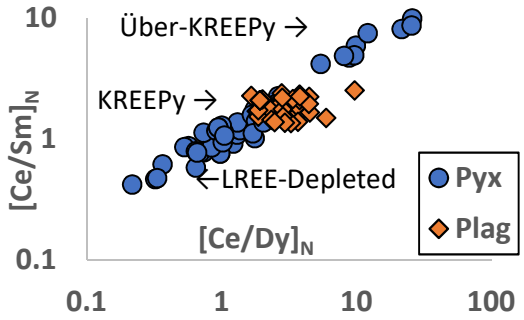

Fig. 2: $[Ce/Y]_N$ vs $[Ce/Sm]_N$ of plagioclase and low-Ca pyroxene equilibrium liquids

An rich. The Apollo 14 KREEP basalts range from An% 63% to 93%, and average around 92%. Apollo 15 KREEP basalts have higher minimum and maximum An% (72% and 98% respectively) but a lower average (83%). Plagioclase within KREEP basalt 72275,136, averaged An:93% (min: 88%, max: 94%).

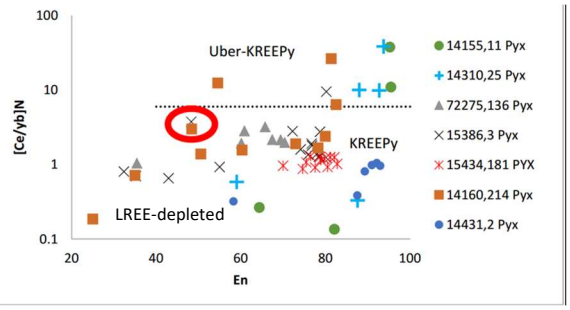

Fig. 3 Pyroxene equilibrium liquids of KREEP basalt plotting enstatite content (En) versus [Ce/Yb]N. As En% decreases so does the LREE enrichment. The red oval notes two pyroxene overgrowths, likely inheriting elevated [Ce/Yb]N ratios from their Über-KREEPy host pyroxene.

Equilibrium liquid REE profiles were calculated for plagioclase and pyroxene [12-15]. Three different equilibrium liquid compositions (2 only found in pyroxenes and one found in plagioclase and pyroxene) are found within KREEP basalts of Apollo 14 and 15, Apollo 17 only has one. (**Fig 2, 3**). 1) über-KREEP is LREE-enriched enriched relative to high-K KREEP [16], has chondritic HFSE/LREE ratios and is from the most Mg-rich pyroxenes, so is likely to be the initial liquid (Apollo 14 and 15). 2) Plagioclase and pyroxene equilibrium liquids similar to high-K KREEP [16], possessing chondritic to supra-chondritic Zr/Hf and HFSE/LREE ratios, and from a variety of pyroxene compositions (Opx to Augite, Apollo 14, 15 and 17). 3) LREE-depleted pyroxene-equilibrium liquids with sub- to supra-chondritic Zr/Hf and HFSE/LREE ratios; typically found in late forming Fe- and Ca-rich pyroxenes (Apollo 14, and 15).

Discussion: Mg-rich pyroxenes typically form early but the elevated ITE's of über-KREEP normally indicate later crystallization, after the ITEs are enriched in the remaining liquid. Ca-and Fe-rich pyroxenes typically form later, however low ITE abundances (from the LREE-depleted pyroxenes) typically indicates early formation. Thus, the constituent equilibrium liquids of KREEP basalts result in a seemingly paradoxical sequence of crystallization. Where the early forming minerals possess REE abundances of late crystallizing minerals, and late forming minerals possess REE abundances of early crystallizing minerals.

To account for this sequence of crystallization we have constructed several models, using fractional crystallization and partial melting, to reproduce the observed equilibrium liquid profiles observed from KREEP basalts (Table 1).

The two models in Table 1 use a orthopyroxenite as the initial solid (Solid-0) that undergoes multiple stages of partial (fractional) melting. Each stage of partial melting produces a residual solid (RS-#) and a melt

Step	3 Stage	2 Stage
Initial solid REE pattern	LREE-depleted	Dilute- high-K KREEP
Partial melting of initial solid	F = 0.005 S1 and RS1 produced	F = 0.01 S1 and RS1 produced
Über-KREEP pyroxenes Crystallize		
Partial melting of RS1	F = 0.06, RS2 and S2-liquid produced	F = 0.10, RS2 and S2-liquid produced
Intermediate crystallization step	--	S2 crystallizes, Whit. Aug. and Plag. F = .85 (15% crystallizes)
--	--	LREE-depleted liquid produced
Mixing of S1 and S2	15%-S1 85%-S2 producing M1: remainder of S1, s2 remains at 66% of original mass	10%-S1 90%-S2 producing M1: S1 is consumed, S2 remains at 21% of initial mass
High-K KREEP like liquid (M1) is produced and KREEPy plagioclase and pyroxene form		
Partial melting of RS2	F = 0.1, produces RS3 and S3	--
Mixing of S2 and S3	LREE-depleted liquid produced M2	--
LREE-depleted Ca-and-Fe-rich Pyroxene form		

Table 1: KREEP basalt modeling. Please see text for discussion. Whit = Whitlockite; Aug = Augite; Plag = Plagioclase

(S#), M# represents mixing where "#" is the 'step' (1, 2 etc.) of partial melting. The ideal visual representation would be REE profiles displaying each step of the model, however there is not enough room to show this in the abstract.

Conclusions: KREEP basalts contain at least three distinct equilibrium liquid compositions: KREEPy (Pyx and Plag); über-KREEPy (Pyx only); and LREE-depleted (Pyx only). When the major element and ITE compositions are examined for each pyroxene results in what seems to be a paradoxical crystallization sequence.

. Modeling shows either two- or three-stages of partial melting can reproduce the REE profiles observed in the treatment basalt pyroxene equilibrium liquids, and will be presented in their full at LPSC 49.

References: [1] Warren P.H. & Wasson J.T. (1977). PLSC 8. [2] Warren P.H. (1988). PLPSC 18. [3] Ryder G. (1987). JGR 92(B4). [4] McKay G.A. et al., (1978) PLPSC 9. [5] Warren P.H. & Wasson J.T. (1980). PLPSC 11. [6] Cronberger K., & Neal C.R. (2012) LPSC 43 #2203. [7] Neal C.R. et al. (2015) GCA 148, 62-80. [8] Cronberger K. & Neal C.R. (2018a) MaPS. [9] Cronberger K. & Neal C.R. (2018b) MaPS. [10] Cronberger K. & Neal C.R. (2017) MaPS, 52(5). [11] Pearce N.J et al., (1997). Geostds. Mewslet., 21(1). [12] Yao L. et al. (2012). Contb. Min & Pet, 164(2). [13] Sun C. & Liang Y. (2013) GCA 119. [14] Bindeman I.N. et al. (1998) GCA 62(7). [15] Putirka K.D. (2008). Rev. Min. Geochem. 69(1). [16] Warren P.H. (1989) LPI Tech. Rpt. 89-03, 149-153.